

Analysis of Parameters Affecting Beam Gauge Performance

S. Yadav, J. Kerby and J.P. Ozelis

Abstract-- Beam gauges have been used in the last decade or so for measuring the internal azimuthal compressive coil stresses in superconducting magnets. In early model LHC quadrupoles tested at Fermilab, the beam gauges indicated excessively high amounts of inner and outer coil prestress during the collaring process, inconsistent with the coil size and modulus data. In response to these measurements, a simple mechanics based quantitative understanding of different factors affecting beam gauges has been developed. A finite element model with contact elements and non-linear material behavior, confirmed with experimental results, was developed. The results indicate that a small plastic deformation of either the beam or the backing plate can cause significant errors in the measured stress values. The effect of variations in coil modulus and support boundary conditions on beam gauge performance are also discussed.

I. INTRODUCTION

Strain gauge based beam-type transducers (beam gauges) have been used since 1989 to measure internal azimuthal compressive coil stresses in superconducting magnets [1,2]. For the LHC IR Quadrupoles being built and tested at Fermilab, beam gauges have been used along with capacitance gauges to measure the internal coil prestress. The gauge packs were located longitudinally in two distinct areas corresponding to the smallest coil size (low prestress) and the largest coil size (high prestress) regions. Table I shows the experimentally measured values of the coil prestress for the inner and outer layers measured at the low prestress region by both the beam and capacitance gauges. Similar measurements for the high prestress region are provided in Table II.

TABLE I

Measured coil prestress for the LHC IR Quad model magnets for the low prestress region.

	Inner layer azimuthal prestress (MPa)		Outer layer azimuthal prestress (MPa)	
	Beam Gauge	Cap Gauge	Beam Gauge	Cap Gauge
	HGQ01	98 ± 3	72 ± 6	70 ± 2
HGQ02	54	66	71 ± 2	
HGQ03	181 ± 27		70 ± 6	92 ± 5
HGQ05		96 ± 3	41 ± 6	
HGQ06		60 ± 4	140 ± 26	70 ± 3
HGQ07		68 ± 1	58 ± 4	70

TABLE II

Measured coil prestress for the LHC IR Quad model magnets for the high prestress region.

	Inner layer azimuthal prestress (MPa)		Outer layer azimuthal prestress (MPa)	
	Beam Gauge	Cap Gauge	Beam Gauge	Cap Gauge
HGQ01	65 ± 5	65	81 ± 18	
HGQ02	82 ± 13	99	99 ± 10	
HGQ03	205 ± 43		127 ± 16	
HGQ05		109	59 ± 5	84
HGQ06		71 ± 5	136 ± 3	66 ± 16

Average of two gauges is provided in the tables along with the standard deviation. The target prestress for the model magnets ranged from 65 to 83 MPa. From Tables I and II, the beam gauge measurements in HGQ03 and HGQ06 indicate excessively large values of the coil prestress (greater than 100 MPa) which are inconsistent with the coil size and modulus data and collared coil deflections. This prompted a combined experimental and numerical investigation in order to understand the various parameters that affect beam gauge performance. The results from such a study are reported in this paper.

II. BACKGROUND

A schematic representation of a beam gauge is shown in Fig. 1. It is comprised of two plates: a thick flat *beam plate* with a strain gauge mounted on it, and a *back plate* which has a notch cut in it to allow bending of the beam. When a pressure P , is applied normal to the beam plate, the beam undergoes bending deformations leading to a change in resistance of the strain gauge.

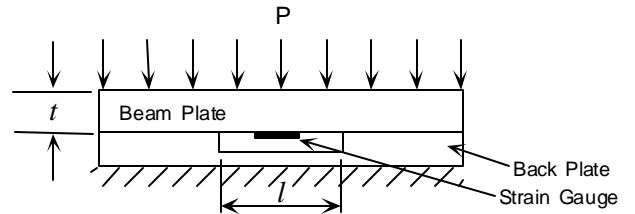


Fig. 1. Beam gauge schematic.

Before being put into the magnet, the beam gauges are calibrated in a fixture (Fig. 2) by measuring the change in

resistance of the gauge for known applied pressures. During calibration while the beam plate is supported by a ten-stack cable, the back plate is rigidly supported in the calibration fixture. A calibration curve relating strain to the applied pressure is obtained.

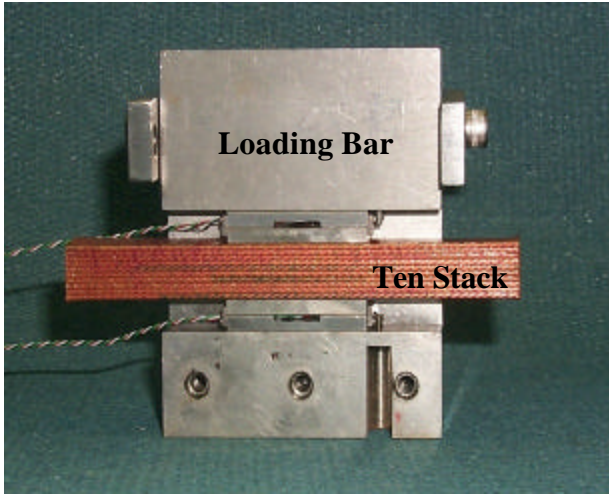


Fig. 2. Calibration fixture for beam gauges.

If l is the length of the beam plate that can undergo bending deformations and t its thickness, then an upper and lower bound can be obtained on the calibration curve depending on whether the beam has fixed ends or simply supported ends. For fixed ends, strain is given by:

$$e = P \frac{l^2}{4 E t^2},$$

whereas for simply supported ends the beam strain is related to the applied pressure by the following formula:

$$e = P \frac{3l^2}{4 E t^2}.$$

In practice, the calibration curve lies in between the two extremes as shown in Fig. 3 for a fixed value of l and t ($l = 12.7$ mm and $t = 4.4$ mm). The observed non-linearity in the calibration curve is due to the non-linear stress-strain behavior of the ten-stack cable.

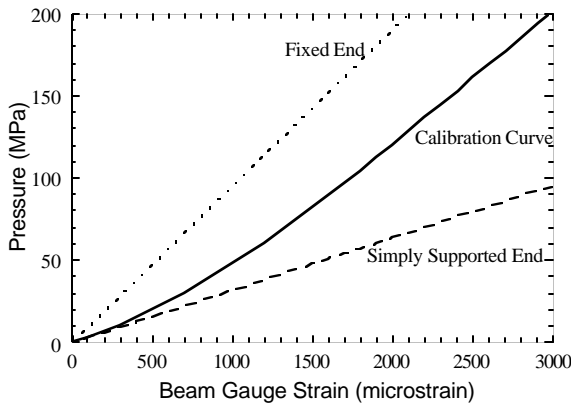


Fig. 3. An actual calibration curve compared to theoretical cases of simply supported and fixed ends for a beam gauge.

A reliable measurement of the coil prestress depends on a calibration methodology that reproduces closely the actual conditions inside a magnet. Several factors that could affect calibration are modulus variation of ten-stack cable, support (boundary) conditions for the beam gauge, and non-linear material behavior. A finite element model (corroborated with experiments) utilizing contact elements and non-linear material behavior has been developed to investigate quantitatively the influence of different factors on beam gauge calibration and performance.

III. EXPERIMENTAL RESULTS

Simple gauge calibration experiments were performed using Ultem[®] 1000 instead of the ten-stack cable normally used for gauges calibrated for use in the model magnets. Ultem[®] 1000 was chosen due to its well-characterized linear stress-strain behavior and also because its modulus of 3.3 GPa is similar to the Young's modulus of coils used in the model magnets. Moreover, the hysteresis in the stress-strain behavior observed during repeated loading/unloading of a ten-stack cable is not observed in Ultem[®] 1000. The maximum stress applied to the Ultem[®] block was always below its yield strength so no plastic deformation occurred in the Ultem[®].

A cross-section of the IR Quad magnets indicating the placement of the inner and outer beam gauges is shown in Fig. 4. For both the inner and outer beam gauges, the beam plate is supported by the coil turns and the back plate is supported by the collar laminations. However, the back plate of the inner beam gauges is not supported rigidly due to the very narrow collar width in the inner pole region. To understand the significance of support (boundary) conditions on gauge performance, calibration experiments were performed for two different gauge configurations (Fig. 5). In the first configuration (called A), the back plate rests on a rigid surface while the load is applied to the beam plate through a block of Ultem[®]. In the second configuration (called B), the back plate rests on an Ultem[®] block while the load is applied to the beam plate through an Ultem[®] block. The above two configurations can be envisioned as a close representation of the two different support conditions for the outer and inner beam gauges.

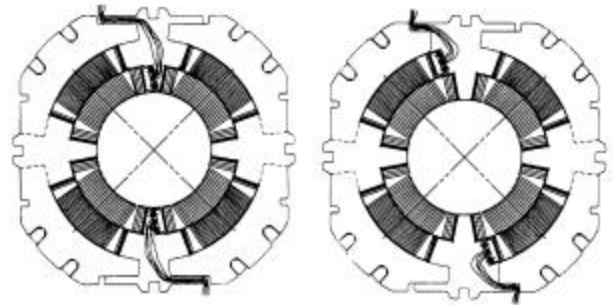


Fig. 4. LHC IR Quadrupole magnet cross-section showing placement of (a) inner beam gauges, and (b) outer beam gauges.

The experimental calibration curves (during loading and unloading) obtained for the two different support configurations are shown in Fig. 5. It is observed that for applied pressures less than 30 MPa, the loading curves for both configurations are almost identical. However, for higher pressures the two loading curves begin to deviate significantly and the same applied pressure causes greater strains for configuration *B*, where the back plate is not rigidly supported. If beam gauges were calibrated in a configuration resembling configuration *A*, yet operate in a configuration similar to configuration *B*, then very large errors would be obtained when computing stress values. This demonstrates the significance of the support conditions in influencing the gauge performance. For both configurations, the unloading does not follow the loading behavior and there is a residual microstrain after complete removal of the applied load. This apparent hysteresis in the loading/unloading behavior is more severe for configuration *B* and the residual microstrain increases with increasing applied load.

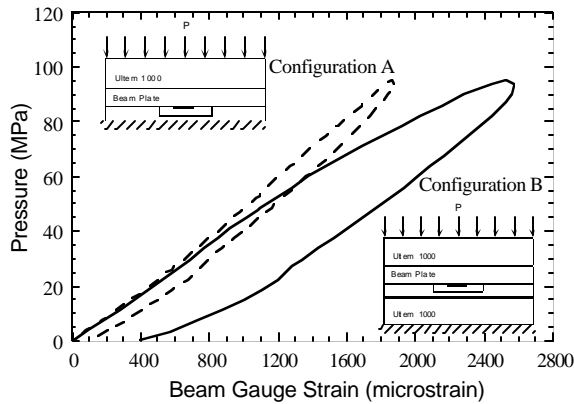


Fig. 5. Comparison of calibration curves obtained from two different support conditions.

IV. FINITE ELEMENT MODELING

A two-dimensional finite element model using ANSYS[®] was developed [3] to understand the observed experimental results. The analysis used 2-D plane quadrilateral elements (PLANE 42) to represent material areas, whereas all contact surfaces were modeled using CONTAC 48 contact elements. The beam and back plates were modeled as Nitronic 40 steel with a Young’s modulus E , of 200 GPa and a Poisson’s ratio ν , of 0.3. The contact stiffness kN of the contact surfaces was determined by the following criteria:

$$kN \approx f E h,$$

where E is the Young’s modulus of the less stiff contacting material, h is the out of plane thickness of the bodies in contact and f is a factor varying between 0.01-100. A value of f equal to 1 was used for the present simulations.

A. Influence of gauge material properties

Finite element solutions are compared with the experimental result for configuration *B* in Fig. 6. The solid curve represents the experimental result. Three different numerical solutions obtained from finite element analysis are presented. The first solution assumed that the beam gauge material remains elastic for all stress states. For this case, the bending strains in the beam increase linearly with the increase in the applied pressure. However, the results do not match well with the experimental results. The second solution assumed bilinear isotropic hardening in the gauge material, using Nitronic 40 steel with a yield strength of 672 MPa and an ultimate tensile strength of 868 MPa. The introduction of non-linearity (plasticity) in the beam gauge material leads to a non-linear numerical solution. When compared to the elastic solution, the same applied pressure causes more bending deformation in the beam gauge for an elastic-plastic gauge material. However, the numerical solution still does not match the experimental result well. Using properties of annealed Nitronic 40 steel, with a yield strength of 413 MPa and an ultimate tensile strength of 800 MPa, as used in early gauges, gives results that match the experimental result extremely well. The results also indicate that very large bending deformations can occur in the beam gauge if the gauge material can deform plastically.

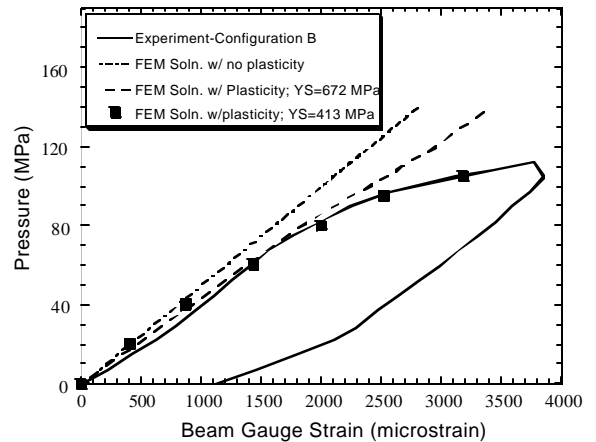


Fig. 6. Comparison of experimental results with finite element solutions.

A contour plot of von Mises stress for the beam gauge in configuration *B* for an applied pressure of 120 MPa is shown in Fig. 7. It is observed that very large stresses, more than the yield strength of the gauge material, are produced in certain regions of the beam and back plates. Moreover, the notches in the back plate act as a source of stress concentration, and result in permanent plastic deformation of the beam and back plates. Therefore, pressure values derived from calibration curves obtained where no plastic deformation of the gauge occurs, give incorrect results.

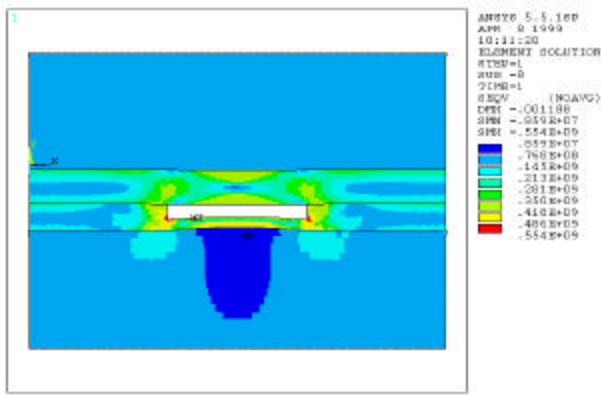


Fig. 7. Contour plot of equivalent von Mises stress for an applied pressure of 120 MPa.

B. Influence of boundary (support) conditions

Several different finite element simulations were performed with different boundary conditions and initial conditions. The simulations demonstrate that the beam and back plate support, and load application affect results significantly. Simulations were performed for the two configurations shown in Fig. 5 with the assumption that the gauge material remains elastic for all stress states. The results show that the difference in the behavior observed in Fig. 5 for the two different configurations is primarily due to the plastic deformation of the gauge material in configuration B. This is due to the fact that if the gauge material is assumed to stay elastic, then both configurations A and B have almost identical calibration curves.

C. Influence of back plate deformations

The contour plot of von Mises stress shown in Fig. 7 indicates that the back plate undergoes much more severe plastic deformation than the beam plate. An attempt was made to understand the role of permanent deformations of the back plate on the calibration behavior. Therefore, a simulation was run for configuration B, where the beam plate was assumed to stay elastic while the back plate could become plastic if the equivalent stresses in the back plate exceeded its yield strength. The results from this simulation showed that even plastic deformation of the back plate could cause a significant change in the calibration behavior. Thus, it is necessary to design beam gauges such that the beam plate and the back plate stay elastic for the entire range of applied pressures.

D. Influence of coil Young's modulus

The finite element model was also used to investigate the effect of changes in the Young's modulus of the Ultem[®] block (representing variations in the Young's modulus of the inner and outer coils in a magnet). It was assumed that the gauge material is elastic and the Young's modulus varied between 3 to 10 GPa. The results are presented in Fig. 8. For coil prestress up to 80 MPa, there is no significant change in the calibration curves with changes in Young's modulus. This indicates that if the beam gauges are designed to stay elastic for operating loads, then the gauge

calibration curves are not very sensitive to the changes in azimuthal modulus of the magnet coils.

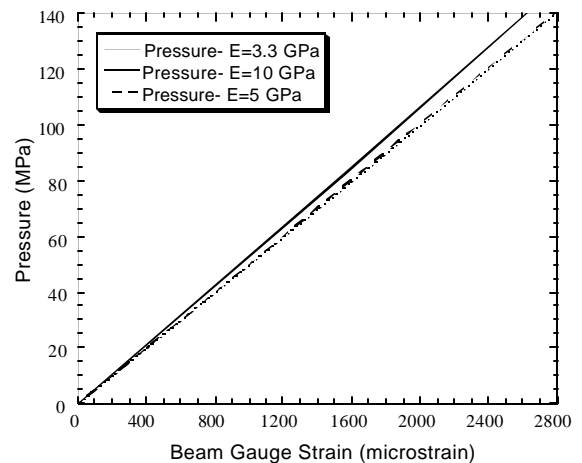


Fig. 8. Effect of Young's modulus of Ultem[®] on calibration.

V. CONCLUSIONS

A finite element model of the beam gauge has been utilized to develop a mechanics based understanding of the parameters affecting beam gauge performance. The main conclusions from this study are summarized below:

- (1) Beam gauge material must be elastic everywhere.
- (2) Elastic behavior of both beam and back plate is important. The plastic deformation (bowing) of only the back plate can lead to large errors when computing stress values.
- (3) Changes in support conditions can increase the chances of plastically deforming the gauge material.
- (4) Coil modulus changes have a small effect on gauge performance.

In light of the current understanding, the early design of the beam gauges was modified beginning with HGQ07. The design changes included a change in gauge material from Nitronic 40 to Nitronic 50 steel with an increased yield strength of 1200 MPa, increasing the thickness of the back plate over the portion that undergoes bending deformations, and reducing the stress concentration at the back plate notches by providing a radius at the sharp corners.

REFERENCES

- [1] C.L. Goodzeit, M.D. Anerella and G.L. Ganetis, "Measurement of internal forces in superconducting accelerator magnets with strain gauge transducers, SSC-MAG-R-7312, (1989).
- [2] M. Davidson, A. Gibertson and M. Dougherty, "Investigation of factors affecting the calibration of strain gage based transducers ('Goodzeit Gages') for SSC magnets," Supercollider 3, edited by J. Nonte, Plenum Press, pp. 1077-1085, (1991).
- [3] S. Yadav and J. Kerby, "On the mechanics of beam gauges," TD-99-026, FNAL, (1999).